Received: 1 August 2022 | Revised: 6 November 2022 | Accepted: 18 November 2022

DOI: 10.1002/gj.4658

RESEARCH ARTICLE

WILEY

Oscillations of a fluvial-lacustrine system and its ecological response prior to the end-Triassic: Evidence from the eastern Tethys region

Ning Lu[1] | Yongdong Wang[1,2] | Yuanyuan Xu[1,3] | Liqin Li[1] | Xiaoping Xie[4] | Mihai Emilian Popa[5,6] | Hongyu Chen[1,3] | Micha Ruhl[7] | Wolfram Michael Kürschner[8]

[1]State Key Laboratory of Palaeobiology and Stratigraphy, Nanjing Institute of Geology and Palaeontology, Chinese Academy of Sciences, Nanjing, China

[2]Nanjing College, University of Chinese Academy of Sciences, Nanjing, China

[3]University of Chinese Academy of Sciences, Beijing, China

[4]School of Geography and Tourism, Qufu Normal University, Rizhao, China

[5]School of Geosciences and Technology, Southwest Petroleum University, Chengdu, China

[6]Faculty of Geology and Geophysics, Doctoral School of Geology, Laboratory of Palaeontology, University of Bucharest, Bucharest, Romania

[7]Department of Geology, Trinity College Dublin, The University of Dublin, Dublin, Ireland

[8]Department of Geosciences, University of Oslo, Oslo, Norway

Correspondence
Yongdong Wang, State Key Laboratory of Palaeobiology and Stratigraphy, Nanjing Institute of Geology and Palaeontology, Chinese Academy of Sciences, Nanjing 210008, China.
Email: ydwang@nigpas.ac.cn

Mihai Emilian Popa, School of Geosciences and Technology, Southwest Petroleum University, Chengdu 610500, China.
Email: mihai@mepopa.com

Funding information
National Natural Science Foundation of China, Grant/Award Numbers: 42202020, 41972120, 42072009; State Key Laboratory of Palaeobiology and Stratigraphy, Grant/Award Numbers: 20191103, 213112

Handling Editor: Z.-Q. Chen

The end-Triassic mass extinction is considered one of the "Big Five" extinction events in the Phanerozoic. However, whether the terrestrial ecosystem began to deteriorate or even collapse prior to the Triassic–Jurassic (Tr-J) transition remains controversial. Compared with the documented data from the western Tethyan region, evidence from the eastern Tethyan realm is limited. We undertake a fitting analysis of the sedimentary system, floral community successions and major geological events of the Xujiahe Formation as reflected by the Qilixia Section, Xuanhan area, northeast Sichuan Basin, China. Our results reveal an oscillating fluvial-lacustrine depositional system during the Late Triassic, with the dominant sedimentary processes mainly controlled by the Indosinian Movement. Beside the sedimentary influence on the Xujiahe Flora, climate changes played a more important role. Fluctuating conditions to cooler and dryer climates at this time promoted diversification of gymnosperms under an overall warm and humid climate setting in the Late Triassic in the Xuanhan area. Superimposed on this oscillating long-term climate state, ecosystem destabilization occurred over 1 million years prior to the Tr–J interval in the Xuanhan study area, possibly in response to the intensified storm and wildfire activity and the following environmental changes. Although the Xujiahe Flora always recovered from the interruption of the tectonic movement, it ultimately collapsed under extreme climatic events and ecological pressures induced by the Late Triassic Central Atlantic Magmatic Province event.

KEYWORDS
Central Atlantic Magmatic Province, end-Triassic mass extinction, floral community succession, sedimentary oscillations, Sichuan Basin

1 | INTRODUCTION

The Triassic-Jurassic transition (Tr–J, 201.36 ± 0.17 Ma, Wotzlaw et al., 2014) is marked by the end-Triassic mass extinction, one of the "Big Five" extinction events of the Phanerozoic (Benton, 1995; Raup & Sepkoski, 1982; Sepkoski, 1981). The biotic turnover, ecological crisis, and environmental background across the Tr–J transition have drawn significant attention over the last decades (Barash, 2015; Hesselbo et al., 2007). The impact of the end-Triassic mass extinction on marine organisms has been extensively documented (e.g., radiolarians, Hallam, 2002; foraminifera, Michalík et al., 2007; ammonites and brachiopods, Tomašových & Siblík, 2007; corals and calcisponges, Stanley Jr. et al., 2018; bivalves, Atkinson et al., 2019). Bio- and chemo-stratigraphic data and stratigraphic correlations of sea-level changes, ocean acidification and release of greenhouse gases (e.g., CO_2, CH_4) suggest this event to be triggered by the breakup of Pangea and particularly by the eruptions of the Central Atlantic Magmatic Province (CAMP) at that time (Marzoli et al., 2004; Van de Schootbrugge et al., 2009; Whiteside et al., 2010; Ruhl et al., 2011, Ruhl et al., 2020; Percival et al., 2017; Capriolo et al., 2020; He et al., 2020). Extreme climatic events caused by significant global warming led to habitat and ecosystem disruption and destruction, with palynological and geochemical data suggesting this to have occurred simultaneously in the terrestrial and marine realms (Cleveland et al., 2008; Götz et al., 2009; Hesselbo et al., 2002; Korte et al., 2019; McElwain et al., 1999; Williford et al., 2009). However, the extinction patterns across this event remain controversial, with some suggestions for multiple extinction events throughout the Late Triassic instead of a single mass extinction at the end of the Late Triassic (Benton, 1986; Hallam, 2002; Lucas & Tanner, 2015, 2018). Considerable controversy derives from the response of terrestrial vegetation to these events. Studies of the plant taxonomic records from Greenland, North America, Europe and Gondwana revealed a significant floral turnover at species and community levels (Belcher et al., 2010; Fowell & Olsen, 1993; Kürschner et al., 2007; Kustatscher et al., 2018; McElwain et al., 1999; McElwain & Punyasena, 2007; Olsen et al., 2002). Other works considered that plant community changes across the Tr–J transition were linked to gradual and adaptive ecological reorganization related to long-term environmental variations, suggesting terrestrial plant changes to be local turnovers rather than those associated with a mass extinction (Cascales-Miñana & Cleal, 2012; Barbacka et al., 2017; Lucas & Tanner, 2018; Zhou et al., 2021). As most studies on the end-Triassic mass extinction were carried out in the western Tethyan realm, especially in Europe and North America, critical insight on global changes, including as recorded in the eastern Tethyan realm, is largely missing.

Terrestrial Tr–J transition sequences are well developed in the Sichuan Basin, southwestern China, representing the most expanded Tr–J strata in the eastern Tethyan realm (Wang et al., 2010). Fundamental studies on regional geology, stratigraphy and palaeontology were previously conducted (Wang et al., 2010), showing abundant and diverse plant fossils, represented by the Xujiahe Flora, in the Upper Triassic sequences of the Sichuan Basin (Huang, 1995; Wang et al., 2010; Ye et al., 1986). The Xujiahe Flora has been suggested to be flourishing under tropical-subtropical hot and humid climatic conditions (Lee, 1964; Ye et al., 1986; Wu, 1983; Sun et al., 1995). In recent years, studies on systematic palaeobotany (Lu et al., 2021; Wang et al., 2015; Xu et al., 2021), palynology (Li et al., 2016, 2018; Liu et al., 2015), as well as sedimentology and geochemistry (Lu et al., 2019; Pole et al., 2018; Shen et al., 2022; Zhu et al., 2017) were conducted for these Upper Triassic sequences of the Sichuan Basin, showing notable temporal variations in climate at that time (Li et al., 2020; Li et al., 2021; Lu et al., 2019; Tian et al., 2016). The environmental evolution during the Late Triassic in the northeastern Sichuan Basin is yet poorly understood, which is critical to provide insight on the level of ecosystem stability, deterioration and/or collapse prior to the Tr–J transition in this region.

Here, we investigate the sedimentary succession and sedimentary features of the Upper Triassic sequences in the northeastern Sichuan Basin, with emphasis on the significance of the macro- and microfloral records related to their depositional context. We aim to reveal the environmental/climatic oscillations and ecological responses during the Rhaetian (Late Triassic) in the northeastern Sichuan Basin, next to discussion on the wider stability of the terrestrial ecosystem prior to the Tr–J transition.

2 | GEOLOGICAL SETTINGS

The Sichuan Basin occurred on the northern frame of the eastern Tethyan realm (Figure 1a). This basin is one of the largest sedimentary basins in southwestern China, covering the eastern Sichuan Province and the majority of Chongqing City (Figure 1b). Its tectonic evolution can be divided into three stages: basement formation, craton basin and foreland basin (Wang et al., 2010). The igneous basement of the Sichuan Basin is Meso-Neoproterozoic in age. The sedimentary cover of the Sichuan Basin recorded a stable craton development stage, as reflected by a set of shallow platform carbonate deposits. When the South China Block, the North China Block and the Songpan-Ganzi Terrane collided during the Late Triassic, the Sichuan foreland basin was formed, and the depositional environment changed from marine to terrestrial (Wang et al., 2010). During this time interval, both the end-Triassic mass extinction and the long-term formation of the Sichuan Basin were accurately, and continuously recorded in the Upper Triassic deposits.

The Upper Triassic sequences of the Sichuan Basin are represented by the Xujiahe Formation, a succession of clastic rocks with abundant coal and gas resources (Wang et al., 2010). The formation is widely distributed and well outcropped on the eastern and northeastern margins of the basin. The Qilixia Section is one of the key and well-known Upper Triassic–Lower Jurassic sections in this area, occurring close to Qili town in Xuanhan County, Dazhou City (Figures 1b,c). The Xujiahe Formation is about 520 m thick, outcropping along the road from Xuanhan to Kaijiang counties. The Xujiahe Formation unconformably overlies the Middle Triassic Leikoupo Formation, and it is conformably overlain by the Lower Jurassic

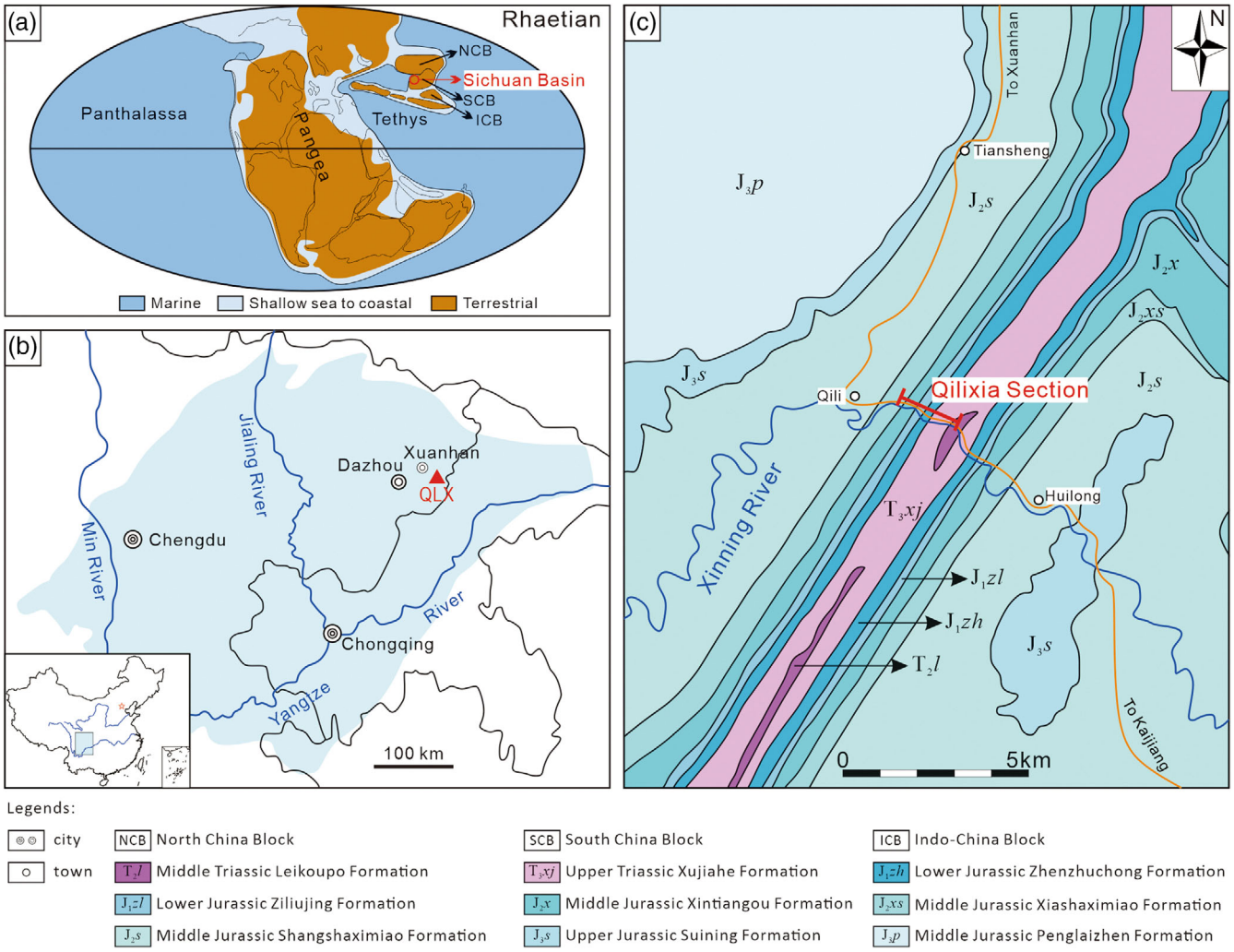

FIGURE 1 Maps showing the location of the Qilixia Section, NE Sichuan Basin, China. (a) The palaeogeographical location of Sichuan Basin during the Rhaetian (Base map after Metcalfe, 2011); (b) The location of the Qilixia Section, NE Sichuan Basin; (c) Simplified geological map of the Qilixia Section and surrounding region (after Wang et al., 2010).

Zhenzhuchong Formation. The Xujiahe Formation is divided into seven members (Members I–VII) with distinct lithological boundaries between each member (Wang et al., 2010). Previous palaeobotanical and palynological data suggest that the Xujiahe Formation is Norian to Rhaetian in age (Li et al., 2016, 2018, 2020; Ye et al., 1986). The combined cyclo- and magneto-stratigraphic record for this section and formation demonstrate that the age of the Xujiahe Formation spans from the latest Norian to the Rhaetian, that is, from 207.2 to 201.3 Ma (Li et al., 2017).

3 | MATERIAL AND METHODS

The Qilixia Section was here studied and sampled for sedimentological investigations. Facies analyses were conducted according to precise sequence data and sedimentary features (Figures 2–4).

Published plant macrofossils of the Xujiahe Formation at the Qilixia Section were compiled and analysed, revealing their ecology (Lu, 2019; Wang et al., 2010; Wu, 1999; Ye et al., 1986), and new plant specimens were collected and supplemented to the previously existing dataset, next to sporomorph data (Li et al., 2016, 2020; Lu et al., 2019).

Photographs of plant fossils were taken with a Nikon® Z7 digital camera with an Z 24–70 mm f/4 S lens. The photographs of plant fossils and lithologies of the Xujiahe Formation were corrected only for contrast and sharpness using Adobe® Photoshop®. The line drawings of some plant fossils were produced using CorelDRAW® 2021. The selected specimens of plant fossils reported and figured here are housed in the Nanjing Institute of Geology and Palaeontology, Chinese Academy of Sciences, Nanjing, China, with catalogue numbers: PB201033-201041.

4 | RESULTS

4.1 | Lithology

The Xujiahe Formation comprises seven lithological members (Members I-VII) in the studied section. Stratigraphic boundaries between each

FIGURE 2 Stratigraphic boundaries and lithologies of the Xujiahe Formation at the Qilixia Section. (a) The lithological boundary between the Upper Triassic Xujiahe Formation and the Middle Triassic Leikoupo Formation; (b) The lithological boundary between the Lower Jurassic Zhenzhuchong Formation and the Upper Triassic Xujiahe Formation; (c) The massive sandstone bed of Member II; (d) The sandstone bed with carbonized branches of Member IV; (e) The mudstone bed with siderite concretions of Member I; (f) The fossils- bearing layers and coal seam of Member VII; G. The conglomerate layer of Member II; (h) The conglomerate layer with tree trunks of Member II.

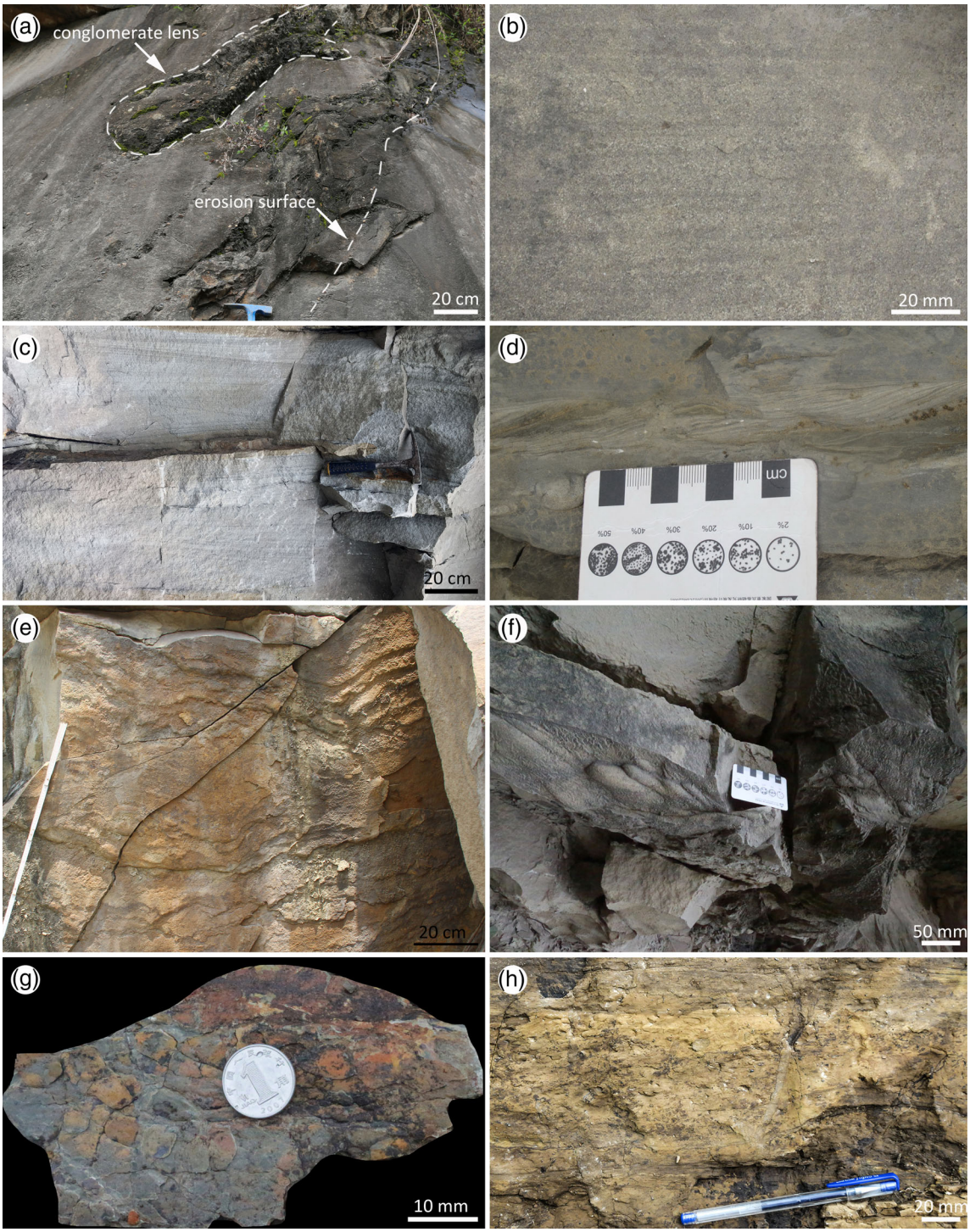

FIGURE 3 Sedimentary structures of the Xujiahe Formation at the Qilixia Section. (a) The sandstone bed with conglomerate lens and erosion surface of Member II; (b) The parallel bedding of Member IV; (c) The cross-bedding of Member VI; (d) The climbing ripples of Member IV; (e) The wave-ripple marks of Member VI; (f) The load casts of Member II; (g) The mud cracks of Member I; (h) The *Skolithos* burrows of Member III (after Pole et al., 2018).

member and bed are distinct, and they are easily recognized through lithological features (Figure 2a,b). The Xujiahe Formation is represented by a succession of dominant sandstone and mudstone beds, while conglomerates, coal seams and thin layers of concretions were also deposited. Rock colours, sedimentary structures, coal accumulation and fossil preservation further reflect the Late Triassic depositional features.

The members II, IV and VI of the Xujiahe Formation are dominated by thick sandstone beds, mostly medium- to fine-grained feldspathic-quartz and quartz sandstone, showing greyish to grey colours (Figure 2c). Carbonized plant branches are preserved in these sandstone beds (Figure 2d). A few coarse sandstone layers occur with quartz and/or chert gravels and with erosional surfaces (Figure 3a).

Cross-bedding is the most frequent and notable structure in the sandstone beds, usually associated with parallel bedding as well (Figure 3b,c). Climbing ripples are recorded in members II and IV (Figure 3d). Wave-ripple marks and load-casts occur in the sandstone of the members II and VI (Figure 3e,f).

The members I, III, V and VII are dominated by grey to black mudstone and silty mudstone beds (Figure 2a,e,f). Variations in colours, between "grey", "dark grey" and "black" are mainly dependent on the organic matter content, beds of these colours were mostly deposited in a coastal marsh (e.g., Member I) or peat swamp (e.g., Member VII), co-existing with coal seams. The horizontal and massive bedding of the mudstone beds are typically indicative of changing hydrodynamics and the supply of terrestrial clastics. Mudstones with preserved root-mucks and mud-cracks in Member I suggest that unconsolidated sediments were once exposed to relatively dry climate conditions (Figures 3g, 5a). The *Skolithos*-type burrows of Member III show a near-shore environment (Figure 3h). Some thin layers of siderite concretions are exposed in the mudstone beds of members I and V (Figure 2e), and two layers of calcic concretions are developed on the top of Member I.

Conglomerate layers are exposed at the bottom of the sandstone beds, and some conglomerate lenses occur within sandstone beds (Figures 2g, 3a). Quartzite and chert pebbles are common in conglomerate layers, indicating a long distance of transportation and/or flushing effects of high-energy flow. Fossil tree trunks are commonly observed in the conglomerate layers as a result of flash flooding, debris flow events (Figure 2h).

Multiple thin coal seams occur in the mudstone members I, III, V and VII (Figure 2a,f), suggesting a reducing environment with abundant clastic sediments. The main industrial coal seams occur in Member VII (Figure 2f), and a few coal seams of Member V also have mining significance. Particularly thin layers of siltstone and muddy siltstone occur as roof and floor shales.

4.2 | Sedimentary facies and environment

The Xujiahe Formation of the Qilixia Section records a fluvial and lacustrine system (Figure 4), while Member I records also a coastal marsh depositional system. These systems could be identified based on facies, subfacies and microfacies characters.

The sandstone members record a well-developed meandering river system (e.g., members II and IV, Figure 4). Associated riverbed microfacies is mainly represented by conglomerate and pebbly sandstone with clear erosional surfaces (e.g., the middle part of bed 04, Member II, Figure 4). The typical retention sediments, including tree trunks and mud inclusions, are usually exposed as lenses at the bottom of erosional surfaces (Figure 3a). The marginal bank (point bar) microfacies are mainly represented by greyish, cross-bedded sandstone (e.g., the upper part of bed 04, Member II, Figure 4). The levee microfacies are developed upward along the marginal banks, depositing fine-grained sandstone and siltstone. Flash floods destroyed levees and formed crevasse splay microfacies. Carbonized branches and mud interlayers are common in the sandstone beds of a crevasse splay (e.g., Figure 2d). The floodplain subfacies are generally developed at the top stage of a meandering river system or lateral it, consisting of siltstone and muddy siltstone. Horizontal beddings are common, and calcic concretions occur locally. The observed peat swamp is developed in a floodplain with limited preservation for channel lateral migration (e.g., bed 10, Member V, Figure 4).

The fluvial delta plain facies expanded into a fluvial-lacustrine transition zone (e.g., Member V, Figure 4). The distributary channel microfacies are mainly represented by fine-grained, well-sorted sandstone. Mud flames and tree trunks are common to the bottom of channel sandstone beds (e.g., bed 10, Member V, Figure 4). The interdistributary bay microfacies are dominated by dark grey to black mudstone and carbonaceous mudstone, interlayered with thin-bedded siltstone. Plant fossils and siderite concretions are common in the interdistributary bay deposits (e.g., the lower part of bed 09, Member V, Figure 4). Peat continuously accumulate in the swamps of a relatively stable delta plain, which represents the important coal accumulating environments (e.g., the upper part of bed 09, Member V, Figure 4).

The lacustrine system include lakeshore and shallow lake subfacies (e.g., bed 16 and the lower part of bed 15, Member VII, Figure 4). However, semi-deep and deep lake subfacies do not develop in the Qilixia Section locality. The lakeshore subfacies are dominated by grey-dark to black mudstone. Industrial coal seams are developed in the lakeshore swamp microfacies, containing fine-grained and thin bedded sandstone and siltstone beds (Figure 2f). The shallow lake subfacies are dominated by thin-bedded grey mudstone, silty mudstone, and muddy siltstone. Some hydrophyte plant taxa (e.g., *Neocalamites*) and bivalves occur in the shallow lake deposits (Huang & Lu, 1992).

According to the occurrence of marine bivalve fossils in the western Sichuan Basin and the occurrence of *Lingula* sp. in the eastern Sichuan Basin, the microfacies of Member I consists of lagoon, coastal marsh and estuarine sandbars (Gou, 1998; Wang et al., 2017; Figure 4), as a result of the transgression and regression cycles during the latest Norian to the Rhaetian (Lu et al., 2015, 2019).

4.3 | Floral community succession

The Xujiahe Flora has been reported throughout the Sichuan Basin, yielding well-preserved and highly diverse fossils, especially for the Qilixia Section and its surrounding areas (Ye et al., 1986; Wang et al., 2010; Figure 5), counting 110 species of 59 genera of plant macrofossils (Ye et al., 1986; Lu, 2019; Figure 6, Table S1). Palynological studies of the Qilixia Section are extensive, reporting a high diversity of spores and pollen, counting 151 species of 64 genera (Li et al., 2016, 2020; Figure 7).

Most of the plant fossils from Member I are too fragmentary to be investigated. According to palynological investigations, the dominant groups in Member I are ferns (52.09% ~ 55.31%), followed by conifers (19.56% ~ 30.17%) and cycads/bennettites/ginkgophytes (8.94% ~ 14.97%) (Figure 8). Some palynomorph

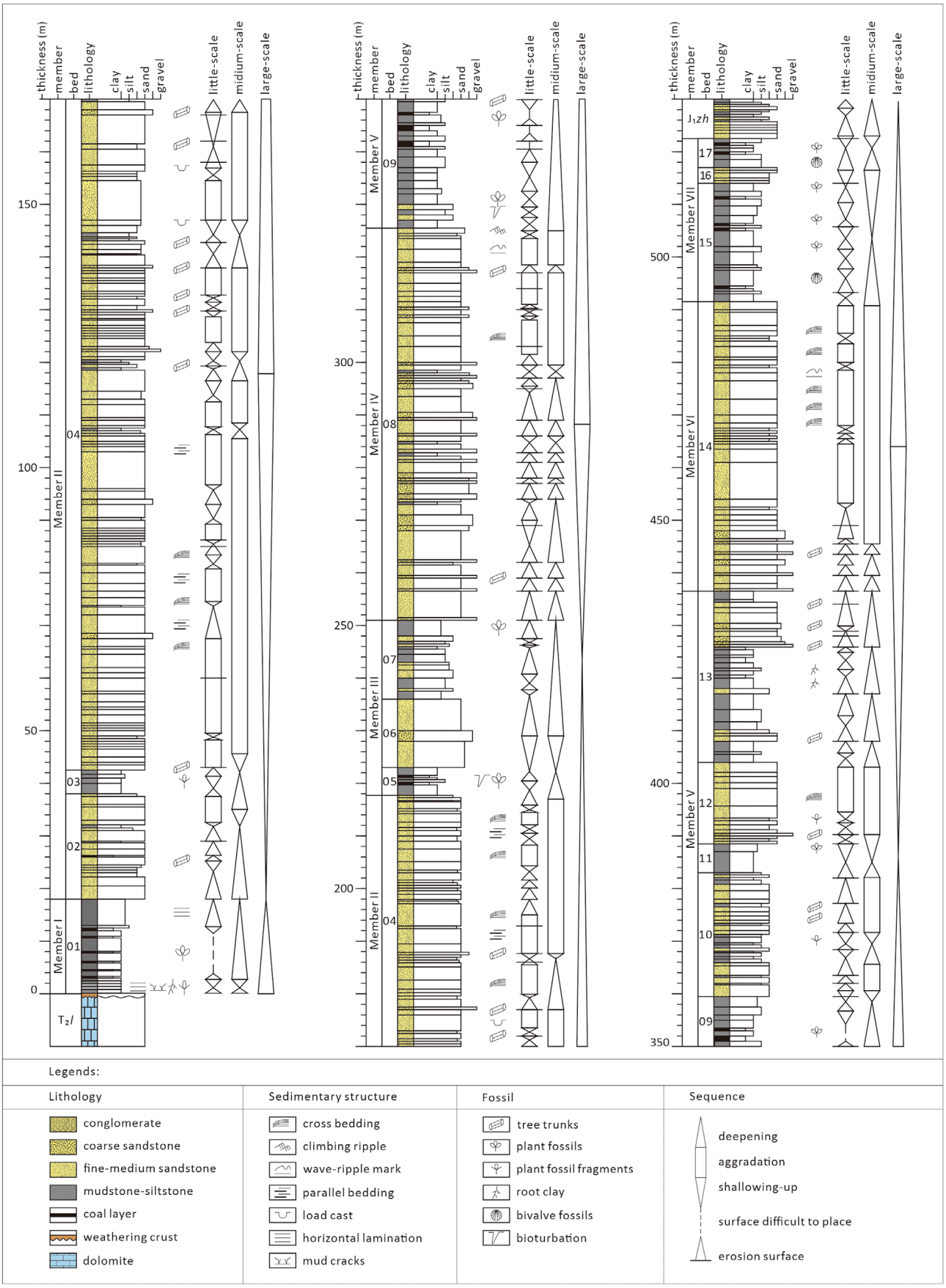

FIGURE 4 Detailed log showing the lithology, sedimentary structures, fossil preservation and sedimentary sequences of the Xujiahe Formation at the Qilixia Section

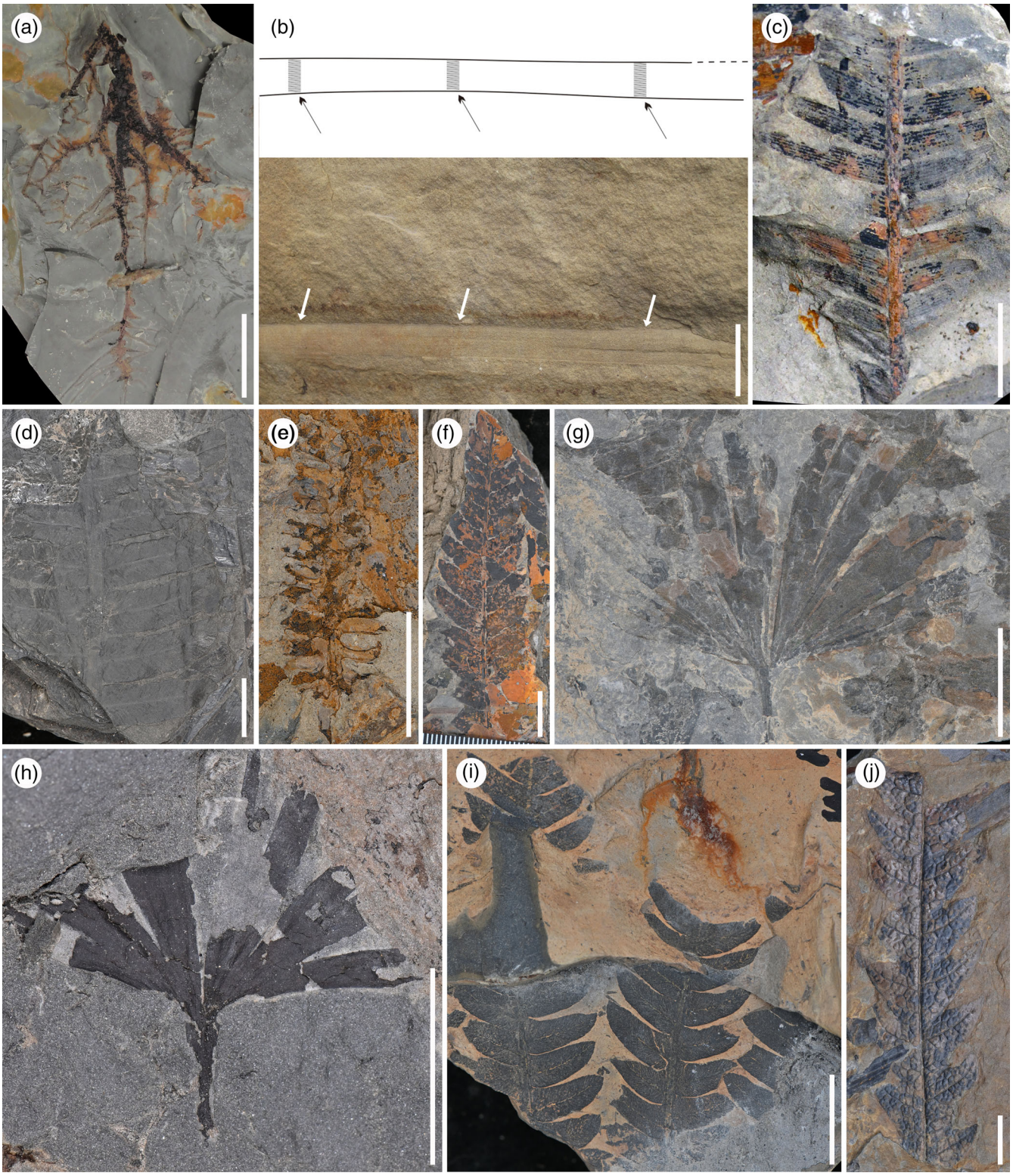

FIGURE 5 Representatives of the Xujiahe Flora collected from the Qilixia Section. (a) *Radicites* sp., Member I, PB201033; (b) *Neocalamites* sp., Member II; (c) *Pterophyllum angustum* (Braun) Gothan, Member V, PB201034; (d) *Cladophlebis raciborskii* Zeiller, Member V, PB201035; (e) *Ixostrobus* sp., Member V, PB201036; (f) *Cladophlebis* sp., Member V, PB201037; (g) *Baiera elegans* Oishi, PB201038; (h) *Ginkgoites sibiricus* (Heer) Seward, Member VII, PB201039; (i) *Cladophlebis* sp., Member VII, PB201040; (j) *Dictyophyllum nathorsti* Zeiller, Member VII, PB201041. ((a), (c)–(j), scale bar = 10 mm; (b) scale bar = 50 mm; The plant fossils are showing in the stratigraphic order).

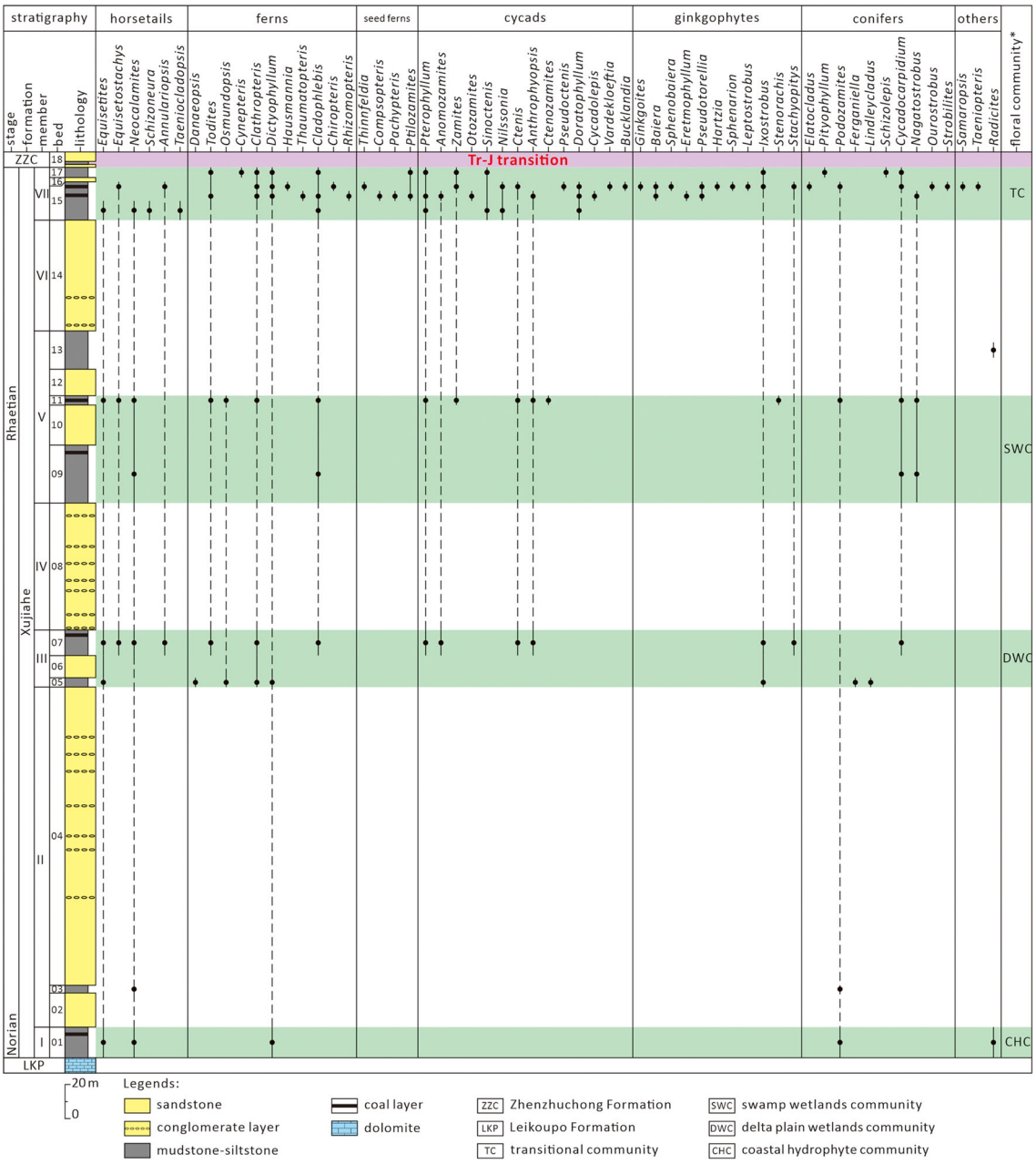

FIGURE 6 Stratigraphic occurrences of the plant macrofossils and division of the floral communities of the late Triassic Xujiahe Flora. *The division of the floral communities are based on the plant macrofossils and palynological data.

environmental indicators (i.e., *Sulcusicystis* sp. and *Radicites* sp.) are also found in Member I (Lu et al., 2015; Li et al., 2016; Figure 5a), all indicating a coastal hydrophyte community (CHC) for Member I at this time (Figure 6).

Plant macrofossils preserved in Member III suggest a community dominated by ferns, cycads, and horsetails (Figure 6, Table S1). The palynological data also indicate a similar community composition, with dominant groups of ferns (51.06% ~ 64.33%) and cycads/bennettites/ginkgophytes (14.33% ~ 15.60%) (Figure 8). The plant macrofossils and palynological data indicate a delta-plain wetland community (DWC) (Li et al., 2020; Lu, 2019). Compared with the CHC of Member I, the diversity of gymnosperms is higher in the DWC of Member III (Lu et al., 2019; Figure 6).

Both macro- and micro-fossils are preserved in the lower beds of Member V (Figures 5c–f and 8). However, the top of Member V yields only macrofossils and no palynomorphs (Figure 8). The dominant groups include ferns (e.g., *Cladophlebis raciborskii*, *Todites* sp., Figure 5d,f), cycads (e.g., *Pterophyllum angustum*, Figure 5c), and ginkgophytes (e.g., *Ixostrobus* sp., Figure 5e). The proportion of fern spores is up to 71.78%, whereas the conifers are only 15.34% (sample QLX-10 of Bed 9, Member V; Figure 8). Both the macro- and micro-fossils indicate a swamp wetland community (SWC) being preserved in Member V (Lu, 2019; Li et al., 2020; Figures 6 and 8).

Most fossil taxa of the Xujiahe Flora were found in Member VII, such as *Dictyophyllum nathorsti*, *Cladophlebis* sp., *Baiera elegans*

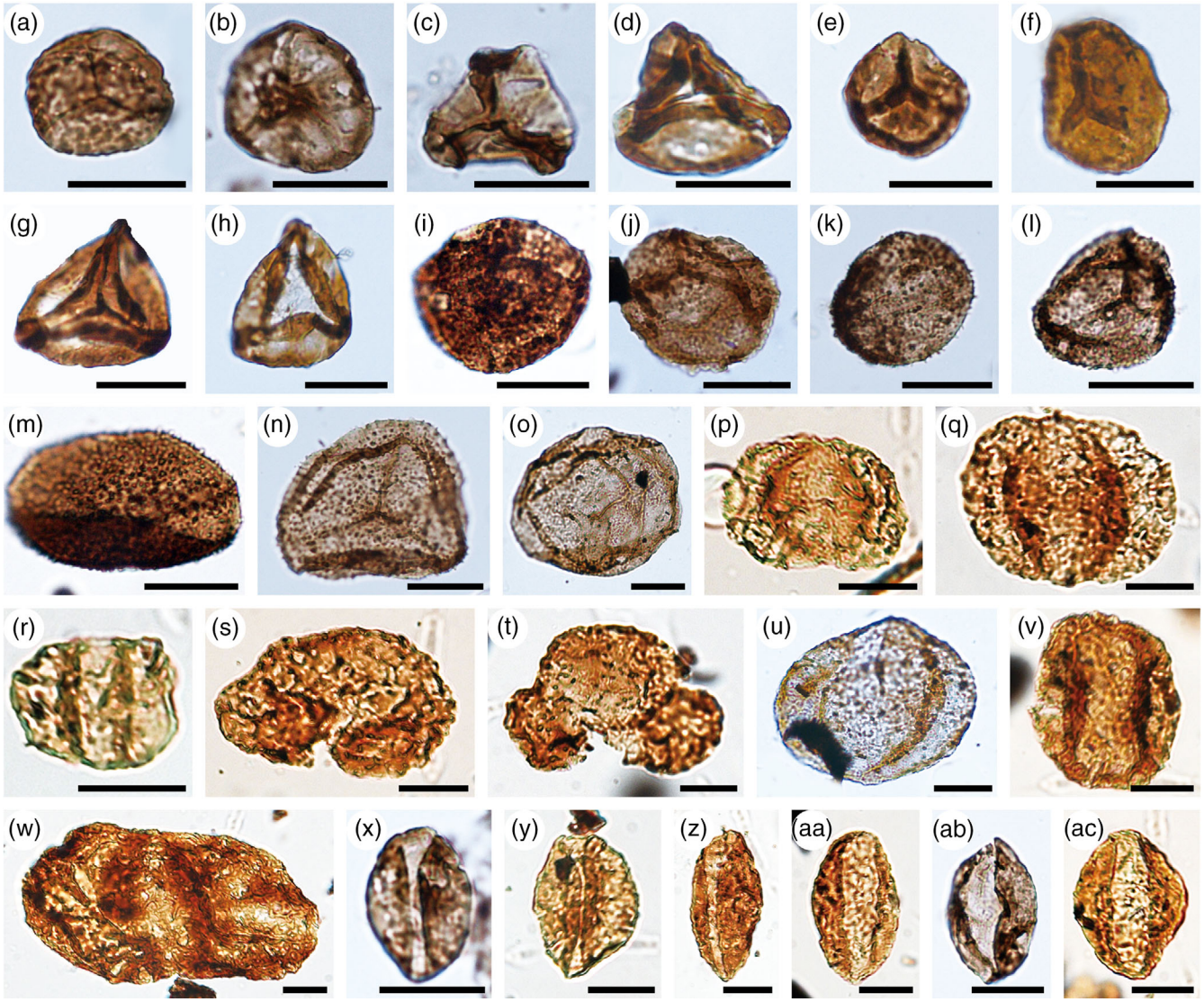

FIGURE 7 Representative spore and pollen taxa recovered from the Xujiahe Formation at the Qilixia Section. (a) *Sphagnumsporites clavus* (Balme, 1957) Huang, 2000, Member I, QLX-1-1; (b) *Sphagnumsporites perforates* (Leschik) Liu, 1986, Member I, QLX-1-4; (c) *Cibotiumspora robusta* Lu et Wang, 1983, Member I, QLX-1-1; (d) *Dictyophyllidites harrisii* Couper, 1958, Member I, QLX-1-1; (e) *Toroisporis minoris* (Nakoman) Sun et He, 1980, Member I, QLX-1-3; (f) *Toroisporis minoris* (Nakoman) Sun et He, 1980, Member III, QLX-7-7; (g) *Concavisporites toralis* (Leschik, 1955) Nilsson, 1958, Member I, QLX-1-3; (h) *Cyathidites minor* Couper, 1953, Member I, QLX-1-4; (i) *Osmundacidites granulata* (Mal.) Zhou, 1981, Member I, QLX-2-1; (j) *Cyclogranisporites arenosus* Madler, 1964, Member III, QLX-8-2; (k) *Angiopteridaspora denticulata* Chang, 1965, Member I, QLX-1-1; (l) *Granulatisporites triconvexus* Staplin, 1960, Member I, QLX-1-4; (m) *Osmundacidites wellmanii* Couper, 1953, Member III, QLX-9-2; (n) *Planisporites dilucidus* Megregor, 1960, Member V, QLX-12-2; (o) *Araucariacites australis* Cookson, 1947, Member I, QLX-1-3; (p) *Alisporites parvus* De Jersey, 1962, Member VII, XHQL-89-5; (q) *Alisporites parvus* De Jersey, 1962, Member VII, XHQL-91-1; (r) *Vitreisporites pallidus* (Reissinger) Nilsson, 1958, Member II, XHQL-40-2; (s) *Pinuspollenites divulgatus* (Bolkh.) Qu, 1980, Member VII, XHQL-91-1; (t) *Pinuspollenites alatipollenites* (Rouse) Liu, 1982, Member VII, XHQL-91-1; (u) *Piceites enodis* Bolkhovitina, 1956, Member II, QLX-2-1; (v) *Quadraeculina anellaeformis* Maljavkina, 1949, Member VII, XHQL-89-1; (w) *Podocarpidites unicus* (Bolkh.) Pocock, 1970, Member II, XHQL-40-1; (x) *Cycadopites parvus* (Bolkh.) Pocock, 1970, Member I, QLX-1-1; (y) *Cycadopites follicularis* Wilson et Webster, 1946, Member II, XHQL-40-2; (z) *Cycadopites reticulata* (Nilsson) Arjang, 1975, Member VII, XHQL-91-1; (aa) *Monosulcites granulatus* Couper 1960, Member VII, XHQL-91-1; (ab) *Monosulcites minimus* Cookson, 1947, Member I, QLX-1-4; (ac) *Monosulcites enormis* Jain, 1968, Member VII, XHQL-89-3. (scale bar = 20 μm).

and *Ginkgoites* sp. (Figure 5g–j). Both species and genera diversity of the plant macrofossils increase at first and then decrease (Figure 6). The dominant groups changed from horsetails to ferns and cycads (Bed 15), and then to ginkgophytes and conifers (Bed 15–17) (Ye et al., 1986; Lu, 2019; Figure 6). Meanwhile, the palynological data also show an upward decrease in ferns and an increase in gymnosperms (e.g., conifers, ginkgophytes) from Bed 15 to Bed 17 (Li et al., 2020; Figure 8). This assemblage change reflects a transitional community succession (TCs), changing from lakeshore swamp to high lands that were preserved in Member VII (Figures 6 and 8).

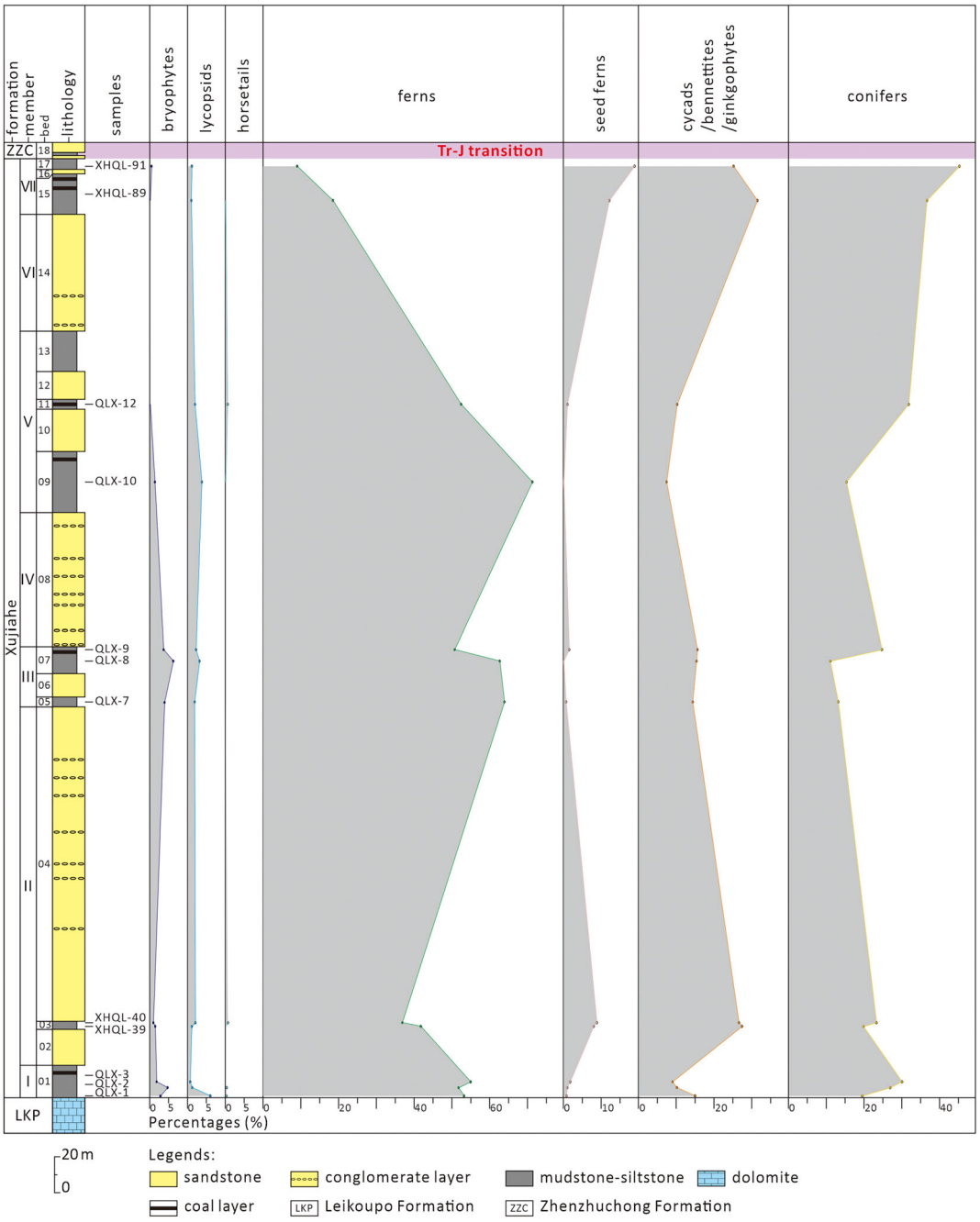

FIGURE 8 Stratigraphic occurrences and abundance diagram of major spore-pollen groups recovered from the Xujiahe Formation at the Qilixia section

5 | DISCUSSION

5.1 | Oscillations between fluvial and lacustrine depositional systems

Significant changes in terms of palaeogeography, palaeoclimate and palaeoecology occurred in the Sichuan Basin throughout the Late Triassic. The Sichuan Basin occurred on the northern margin of the South China Block during the Late Triassic (Figure 1a). With the convergence of the South China Block, the North China Block, and the Indo-China Block (known as the Indosinian Movement), the Sichuan Basin was raised during the Middle to Late Triassic (Zhong, 1998). Due to the uplift of the Sichuan Basin, the westward retreat of the Tethys occurred, and the Middle Triassic Leikoupo Formation was weathered during the Middle to Late Triassic in the Xuanhan area (Deng, 1996; Wang et al., 2010; Zhong, 1998). This large-scale regression was recorded by the sedimentary gap between the Middle Triassic Leikoupo Formation and the Upper Triassic Xujiahe Formation (Figure 2a).

Following the large-scale regression, a new transgressive episode started in the Carnian and influenced the Xuanhan area in the latest

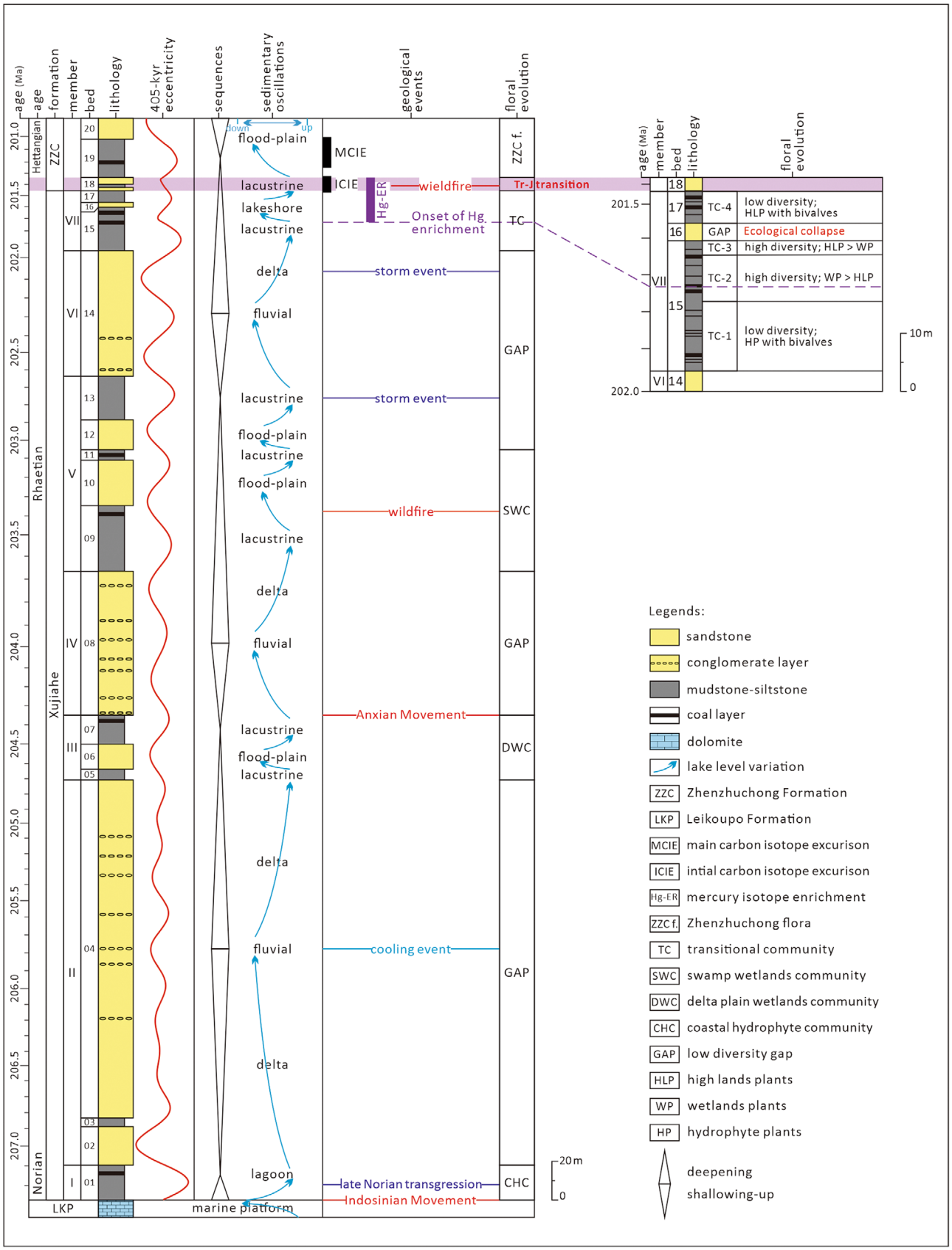

FIGURE 9 Environmental oscillations and the ecological responses of the Xujiahe Formation at the Qilixia Section. (1). The 405-kyr eccentricity cycle and ages are from Li et al., 2017. (2). The initial- and main- carbon isotope excursions and mercury (Hg) isotope enrichment are from Shen et al., 2022.

Norian (Lu et al., 2015). Thereafter, a coastal marsh began to take shape and the Xujiahe Formation was deposited unconformably over the Leikoupo Formation remains (Figure 2a). Some thin layers of coal were accumulated, with the coincidental formation of calcic concretions and gypsum in Member I deposits, indicating a hot climate (Lu et al., 2015).

With the continuous northward compression of the northern margin of the South China Block, the Qinling Orogen to the north of the Sichuan Basin became raised, and rivers originating from the Qinling Orogen started to shape the topography of the Xuanhan area with sufficient terrigenous clastic sediments and water. The meandering rivers became the dominant sedimentary environment, as represented by the sequences of Member II. Repeated flood events, inferred from the regular occurrence of riverbed-point bar-natural levee associations, suggest regular heavy rain events in response to a megamonsoon development (Parrish & Peterson, 1988; Tian et al., 2016) (Figure 9).

With the initial formation of the Sichuan Basin and the continuous deepening of the water at the study locality, the transition from channel to floodplain to lakeshore swamp was recorded in Member III (Figures 4 and 9). However, the relatively stable environment did not last long before the start of another episode of the Indosinian Movement (also known as the Anxian Movement, Wang, 1990). The tectonic activities not only promoted the continuous uplift of the Qinling Orogen, but also resulted in the uplift of the Longmenshan mountains, forming a prominent syntectonic conglomerate sequence near the source area (He, 2014; Liu et al., 2021; Wang, 2003). The fluvial dynamics of the surrounding orogens were therefore enhanced, providing sufficient terrigenous clastic sediments and water. The facies association of Member IV of the Qilixia Section recorded the Anxian Movement and its impact from a distance (Figure 4).

With tectonic activities tending to moderate, the environment became stable, and the lake level became raised (Figure 9). The wide deltaic flood-plain was formed in the middle Rhaetian (ca. 203 ~ 203.5 Ma, Figure 9), with distributary channels and interdistributary bay deposits (Figures 4 and 9). The coal accumulation was enhanced in the stable peat swamp of the interdistributary bay environment, and some thick, industry grade coal seams developed in the lower mudstone beds of Member V (e.g., upper part of Bed 9, Figure 4).

Subsequently, the environment became disturbed again, as suggested by the mudstone breccia of the upper beds of Member V. The mudstone breccia composed of angular boulders suggests either an exceptional storm or even a tsunami event (Pole et al., 2018). Under this disturbed environmental background, very few plant fossils could be preserved. Root clay and siderite concretions occurred in the upper beds of Member V, suggesting fluctuations in the lake level (Figure 9). The disturbed environmental conditions extended throughout the upper Member V and the Member VI. The occurrence of both hummocky and swaley cross beddings in Member VI was proposed as strong evidence of more stormy conditions (Pole et al., 2018). The fine-grained and well-sorted quartz sandstone with wave-ripple marks of the Member VI may suggest a wave-dominated, near-shore environment.

Influenced by the lake transgression, a stable lakeshore and shallow lake environment developed prior to the Tr–J transition (Figure 9). The depositional environment and facies evolution were mainly controlled by lake level changes. With the fall of lake level, a peat swamp environment occurred and the Xuanhan area became the coal depocenter, with industry grade, thick coal seams accumulated related to the stable environmental conditions of Member VII (Figure 2f).

5.2 | Palaeoclimate implications and ecological response

Species diversity, community composition and dominant taxa of the fossil assemblages can allow for inferences on palaeoclimate variations and palaeo-ecosystem stability (McElwain et al., 2007). Furthermore, syntheses of the sedimentary systems, community succession and major geological events contribute to a better understanding of the ecological response of the Xujiahe Flora to the end-Triassic mass extinction and associated climatic and environmental change at that time (Figure 9).

The observed water-level transgression across the wider depositional environment resulted in the formation of a transitional environment, which provided the initial habitats for the rise of the Xujiahe Flora in the latest Norian (ca. 207 ~ 207.2 Ma, Figure 9). The thriving CHC of Member I marked the origin of the Xujiahe Flora in the latest Norian in the Xuanhan area. Both the community composition and the dominant taxa indicate hot and humid climatic conditions (Lu et al., 2019).

Subsequently, an environmentally disturbed floodplain developed during the uplift of the Qinling orogen across the Norian–Rhaetian transition (ca. 205 ~ 207 Ma, Figure 9), terminating the favourable habitats for terrestrial plant ecosystems as described above. Locally, only the sphenopsid *Neocalamites* survived and became the dominant element, but *Podozamites* leaves, mainly transported and buried in the banks of lakes or marshes, indicate a nearshore hydrophyte ecosystem as preserved in Member II (Huang & Lu, 1992). The occurrence of the fossil wood *Xenoxylon guangyuanensis* in the neighbouring region of this basin was notable (Tian et al., 2016). Previously, evidence suggests that the genus *Xenoxylon* was mainly distributed in the high latitude regions and reflecting cool and/or wet climate conditions, the southernmost occurrences of *Xenoxylon* in regions otherwise under warm or dry palaeoclimates might indicate global colder/wetter climatic snaps (Philippe et al., 2009; Philippe & Thévenard, 1996). Therefore, the *X. guangyuanensis* would suggest a climatic cooling event linked to the development of the Late Triassic megamonsoon (Tian et al., 2016), influencing the evolution of gymnosperms.

Nearshore peat swamps developed as a result of lake level rise (Figure 9). A community dominated by ferns, cycads and horsetails was thriving for a short period of time during the early Rhaetian (ca. 204.5 Ma, Figure 9). The occurrence of ginkgophyte fossils (*Stachyopitys*) indicates that the climate was not as hot as during the latest Norian, and the delta plain wetlands community (DWC) of Member III represented the rise of the Xujiahe Flora in the early Rhaetian (Lu et al., 2019).

The second gap, induced by the Anxian Movement, influenced the floral communities again (Member VI, Figure 9), coeval with the uplift of the Longmenshan mountain range towards the southwest, blocking the warm, moist water flow from the Tethys Ocean, deeply reshaping local humidity patterns and the regional climate (Lu, 2019).

In the Middle Rhaetian (ca. 203 ~ 203.5 Ma, Beds 9 and 11 of Member V, Figure 9), ferns and cycads were still dominant (Figures 6 and 8). The ratio of fern spores was even as high as 71.78%, whereas the conifer pollen is only 15.34% (sample QLX-10 of Bed 9, Member V; Figure 8). Both the macro- and micro- fossils indicate a swamp wetlands community (SWC) of the lower beds of Member V, growing under a warm and humid climate. Although the conifers and ginkgophytes showed higher diversity than the CHC of Member I and the DWC of Member III (Figure 6), the abundance was still low, and they were not the dominant groups.

Community destabilization marked the third gap in the floral succession at the study locality, suggesting a precursor interval of environmental stress in the late Rhaetian (ca. 202 ~ 203 Ma, Figure 9). The mudstone breccia of Member V and the occurrence of both hummocky and swaley cross beddings in Member VI recorded the stormy conditions (Pole et al., 2018). The detrital charcoal fragments and inertinite recovered from the samples of the Xujiahe Formation also indicate a disturbed environment marked by intensive wildfire events (Lu, 2019; Pole et al., 2018). This ecosystem disturbance is also indicated by a series of discrete spikes in sulphide content and changes in planktonic community composition in the Panthalassic Ocean prior to the Tr–J boundary (Schoepfer et al., 2022).

Until the terminal Rhaetian, a stable nearshore environment became the refuge of the Xujiahe Flora in the Xuanhan area. Not only did the favourable habitats permit the prosperity of the ferns, but also, it contributed to the diversification of conifers and ginkgophytes. Unlike the communities of the underlying members, the transitional community successions (TCs) of Member VII showed an upward non-uniformity (Figures 6, 8, and 9). Some hydrophyte taxa (e.g., *Neocalamites*) were preserved in the lowermost mudstone layers (TC-1), co-existing with some bivalve fossils (Huang & Lu, 1992; Ye et al., 1986). With the drop of the lake level, the shallow lake retreated and the lake shoreline changed, with the lakeshore subfacies becoming dominant. Within the lakeshore swamp microfacies, the wetland taxa became dominant in the Xuanhan area (TC-2). With the continuous drop in the lake level, the river dynamics became the main sedimentary feature and the flood plain expanded. Both the highland and the wetland taxa (i.e., conifers, ferns) were diverse and abundant in the middle mudstone layers of Member VII (TC-2, 3). The bivalve fossils demonstrate the rise of lake level in the topmost bed of Member VII (Huang & Lu, 1992; Ye et al., 1986), with only a low-diversity floral community dominated by some upland xerophytic taxa (TC-4). The floral associations of the Member VII show an ecological collapse to the end of the Rhaetian (ca. 201.5 ~ 202 Ma, Figure 9).

It is notable that the turnover from TC-2 to TC-3 and the ecological collapse are correlated with mercury enrichment prior to the Tr–J transition, as a CAMP global influence (Shen et al., 2022) (Figure 9). Previous studies proposed that the Central Atlantic Magmatic Province (CAMP) volcanism have increased the frequency and scale of extreme climatic events (Belcher et al., 2010; McElwain et al., 1999, 2007), so that the enormous ecological pressure ultimately destroyed the terrestrial flora and generally their ecosystems (Capriolo et al., 2020; Lindström et al., 2017; Mander et al., 2013; McElwain et al., 1999, 2007; Steinthorsdottir et al., 2012; Yager et al., 2021). Recently, wildfire events across the Tr–J interval were identified at the Qilixia Section and throughout the whole basin (Lu, 2019; Pole et al., 2018; Song et al., 2020). Moreover, a multiproxy analysis (including organic carbon isotopes, mercury (Hg) concentrations and isotopes, the chemical index of alteration (CIA), and clay minerals) of the Xujiahe Formation, across the Tr–J interval at Qilixia Section was undertaken (Shen et al., 2022). The increasing CIA in association with Hg peaks was interpreted as results of reflecting the volcanism-induced intensification of continental chemical weathering, which were linked with the CAMP event (Shen et al., 2022). Therefore, the ecological collapse at the end of the Rhaetian in the Xuanhan area was suggested to be largely induced by the CAMP emplacement and its associated climatic effects.

6 | CONCLUSIONS

1. The Upper Triassic Xujiahe Formation yields the best record of the major changes in palaeogeography, palaeoclimate and palaeoecology occurring in the Late Triassic of the northeastern Sichuan Basin, South China. The oscillating fluvial-lacustrine depositional system during the late Triassic, and the sedimentary evolution of the basin were mainly controlled by the Indosinian Movement and the regression-transgression cycle.
2. Within an overall warm and humid climate during the Late Triassic in the Xuanhan area, some climatic variations occurred, as inferred from differences in floral communities of each member. The cooling and drying fluctuations influenced the diversification of gymnosperms.
3. Four communities and three obvious gaps document the rise and demise of Xujiahe Flora throughout the Late Triassic in the northeast Sichuan Basin. The floral community successions were closely related to sedimentary processes and to climatic variations. An ecosystem destabilization occurred in the Xuanhan area over 1 million years prior to the Tr–J interval, followed by an ecological collapse occurring at the Tr–J interval.
4. The Xujiahe Flora always recovered from the interruptions induced by tectonic movement, and it ultimately collapsed under the extreme climatic events and ecological pressure induced by the CAMP event.

AUTHOR CONTRIBUTIONS

Yongdong Wang, Mihai Emilian Popa and Ning Lu designed the study. Ning Lu, Yuanyuan Xu, Liqin Li, Hongyu Chen, Xiaoping Xie, Micha Ruhl, Mihai Emilian Popa, Wolfram Michael Kürschner and Yongdong Wang carried out the field works. Ning Lu, Yuanyuan Xu and Liqin Li

performed the lab works. Ning Lu, Yuanyuan Xu, Liqin Li and Yongdong Wang wrote the draft. All authors contributed to the interpretation and revision of the manuscript.

ACKNOWLEDGEMENTS

We appreciate Prof. Evelyn Kustatscher for carefully reviewing the manuscript and made helpful comments and suggestions. We would like to thank Prof. Yue Li from Nanjing Institute of Geology and Palaeontology, Chinese Academy of Sciences for the suggestions regarding the manuscript. We appreciate Dr. Mingsong Li from Peking University and Senior Engineer Shuna Xi from the No. 137 Geological Survey of the Sichuan Coalfield Geology Bureau for their kind assistance during fieldtrips.

FUNDING INFORMATION

This study is financially supported by the National Natural Science Foundation of China (42202020, 41790454, 41972120 and 42072009), the Stratigraphic Priority Program (B) of the Chinese Academy of Sciences (XDB2600000), and the Grants from State Key Lab of Palaeobiology and Stratigraphy (20191103, 213112).

CONFLICT OF INTEREST

The authors declare that the research was conducted in the absence of any commercial or financial relationships that could be construed as a potential conflict of interest.

PEER REVIEW

The peer review history for this article is available at https://publons.com/publon/10.1002/gj.4658.

DATA AVAILABILITY STATEMENT

The data that support the findings of this study are available from the corresponding author upon reasonable request.

ORCID

Yongdong Wang https://orcid.org/0000-0002-2873-9427
Micha Ruhl https://orcid.org/0000-0001-8170-0399
Wolfram Michael Kürschner https://orcid.org/0000-0001-6883-6486

REFERENCES

Atkinson, J. W., Wignall, P. B., Morton, J. D., Aze, T., & Hautmann, M. (2019). Body size changes in bivalves of the family Limidae in the aftermath of the end-Triassic mass extinction: The Brobdingnag effect. *Palaeontology*, *62*(4), 561–582. https://doi.org/10.1111/pala.12415

Barash, M. S. (2015). Abiotic causes of the great mass extinction of marine biota at the Triassic-Jurassic boundary. *Oceanology*, *55*(3), 374–382. https://doi.org/10.1134/s0001437015030017

Barbacka, M., Pacyna, G., Kocsis, Á. T., Jarzynka, A., Ziaja, J., & Bodor, E. (2017). Changes in terrestrial floras at the Triassic-Jurassic boundary in Europe. *Palaeogeography, Palaeoclimatology, Palaeoecology*, *480*, 80–93. https://doi.org/10.1016/j.palaeo.2017.05.024

Belcher, C. M., Mander, L., Rein, G., Jervis, F. X., Haworth, M., Hesselbo, S. P., Glasspool, I. J., & McElwain, J. C. (2010). Increased fire activity at the Triassic/Jurassic boundary in Greenland due to climate-driven floral change. *Nature Geoscience*, *3*(6), 426–429. https://doi.org/10.1038/ngeo871

Benton, M. J. (1986). More than one event in the late Triassic mass extinction. *Nature*, *321*(6073), 857–861. https://doi.org/10.1038/321857a0

Benton, M. J. (1995). Diversification and extinction in the history of life. *Science*, *268*(5207), 52–58. https://doi.org/10.1126/science.7701342

Capriolo, M., Marzoli, A., Aradi, L. E., Callegaro, S., Dal Corso, J., Newton, R. J., Mills, B. J. W., Wignall, P. B., Bartoli, O., Baker, D. R., Youbi, N., Remusat, L., Spiess, R., & Szabó, C. (2020). Deep CO_2 in the end-Triassic Central Atlantic Magmatic Province. *Nature Communications*, *11*(1), 1670. https://doi.org/10.1038/s41467-020-15325-6

Cascales-Miñana, B., & Cleal, C. J. (2012). Plant fossil record and survival analyses. *Lethaia*, *45*(1), 71–82. https://doi.org/10.1111/j.1502-3931.2011.00262.x

Cleveland, D. M., Nordt, L. C., Dworkin, S. I., & Atchley, S. C. (2008). Pedogenic carbonate isotopes as evidence for extreme climatic events preceding the Triassic-Jurassic boundary: Implications for the biotic crisis? *Geological Society of America Bulletin*, *120*(11–12), 1408–1415. https://doi.org/10.1130/b26332.1

Deng, K. (1996). Formation and development of Sichuan Basin. In Z. Guo (Ed.), *Sichuan Basin formation and development* (pp. 113–138). Geilogical Publishing House.

Fowell, S. J., & Olsen, P. E. (1993). Time calibration of Triassic/Jurassic microfloral turnover, eastern North America. *Tectonophysics*, *222*(3–4), 361–369. https://doi.org/10.1016/0040-1951(93)90359-r

Götz, A. E., Ruckwied, K., Pálfy, J., & Haas, J. (2009). Palynological evidence of synchronous changes within the terrestrial and marine realm at the Triassic/Jurassic boundary (Csővár section, Hungary). *Review of Palaeobotany and Palynology*, *156*(3–4), 401–409. https://doi.org/10.1016/j.revpalbo.2009.04.002

Gou, Z. (1998). The bivalve faunas from the upper Triassic Xujiahe formation in the Sichuan Basin. *Sedimentary Facies and Palaeogeography*, *18*(2), 20–29.

Hallam, A. (2002). How catastrophic was the end-Triassic mass extinction? *Lethaia*, *35*(2), 147–157. https://doi.org/10.1080/002411602320184006

He, L. (2014). Permian to late Triassic evolution of the Longmen Shan Foreland Basin (Western Sichuan): Model results from both the lithospheric extension and flexure. *Journal of Asian Earth Sciences*, *93*, 49–59. https://doi.org/10.1016/j.jseaes.2014.07.007

He, T., Dal Corso, J., Newton, R. J., Wignall, P. B., Mills, B. J. W., Todaro, S., di Stefano, P., Turner, E. C., Jamieson, R. A., Randazzo, V., Rigo, M., Jones, R. E., & Dunhill, A. M. (2020). An enormous sulfur isotope excursion indicates marine anoxia during the end-Triassic mass extinction. *Science Advances*, *6*(37), eabb6704. https://doi.org/10.1126/sciadv.abb6704

Hesselbo, S. P., McRoberts, C. A., & Pálfy, J. (2007). Triassic–Jurassic boundary events: Problems, progress, possibilities. *Palaeogeography, Palaeoclimatology, Palaeoecology*, *244*(1), 1–10. https://doi.org/10.1016/j.palaeo.2006.06.020

Hesselbo, S. P., Robinson, S. A., Surlyk, F., & Piasecki, S. (2002). Terrestrial and marine extinction at the Triassic-Jurassic boundary synchronized with major carbon-cycle perturbation: A link to initiation of massive volcanism? *Geology*, *30*(3), 251–254. https://doi.org/10.1130/0091-7613(2002)030<0251:Tameat>2.0.Co;2

Huang, Q. (1995). Palaeoclimate and coal-forming characteristics of the late Triassic Xujiahe stage in northern Sichuan. *Geological Review*, *41*(1), 92–99.

Huang, Q., & Lu, S. (1992). The primary studies on the Palaeoecology of the late Triassic Xujiahe Flora in eastern Sichuan. *Earth Science - Journal of China University of Geosciences*, *17*(3), 329–335.

Korte, C., Ruhl, M., Ullmann, C. V., & Hesselbo, S. P. (2019). Chemostratigraphy across the Triassic–Jurassic boundary. In A. N. Sial, C. Gaucher,

M. Ramkumar, & V. P. Ferreira (Eds.), *Chemostratigraphy across major chronological boundaries* (pp. 185–210). American Geophysical Union.

Kürschner, W. M., Bonis, N. R., & Krystyn, L. (2007). Carbon-isotope stratigraphy and palynostratigraphy of the Triassic–Jurassic transition in the Tiefengraben section — Northern calcareous Alps (Austria). *Palaeogeography, Palaeoclimatology, Palaeoecology*, *244*(1), 257–280. https://doi.org/10.1016/j.palaeo.2006.06.031

Kustatscher, E., Ash, S. R., Karasev, E., Pott, C., Vajda, V., Yu, J., et al. (2018). Flora of the Late Triassic. In H. T. Lawrence (Ed.), *The Late Triassic World* (pp. 545–622). Springer.

Lee, P.-C. (1964). Fossil plants from the Hsuchiaho series od Kwangyüan, northern Szechuan. *Memoirs of Institute of Geology and Palaeontology, Academia Sinica*, *3*, 101–178.

Li, J., Huang, C., Wen, X., & Zhang, M. (2021). Mesozoic paleoclimate reconstruction in Sichuan Basin, China: Evidence from deep-time paleosols. *Acta Sedimentologica Sinica*, *39*(5), 1157–1170. https://doi.org/10.14027/j.issn.1000-0550.2020.058

Li, L., Wang, Y., Kürschner, W. M., Ruhl, M., & Vajda, V. (2020). Palaeovegetation and palaeoclimate changes across the Triassic–Jurassic transition in the Sichuan Basin, China. *Palaeogeography, Palaeoclimatology, Palaeoecology*, *556*, 109891. https://doi.org/10.1016/j.palaeo.2020.109891

Li, L., Wang, Y., Liu, Z., Zhou, N., & Wang, Y. (2016). Late Triassic palaeoclimate and palaeoecosystem variations inferred by palynological record in the northeastern Sichuan Basin, China. *PalZ*, *90*(2), 327–348. https://doi.org/10.1007/s12542-016-0309-5

Li, L., Wang, Y., Vajda, V., & Liu, Z. (2018). Late Triassic ecosystem variations inferred by palynological records from Hechuan, southern Sichuan Basin, China. *Geological Magazine*, *155*(8), 1793–1810. https://doi.org/10.1017/s0016756817000735

Li, M., Zhang, Y., Huang, C., Ogg, J., Hinnov, L., Wang, Y., Zou, Z., & Li, L. (2017). Astronomical tuning and magnetostratigraphy of the upper Triassic Xujiahe formation of South China and Newark supergroup of North America: Implications for the late Triassic time scale. *Earth and Planetary Science Letters*, *475*, 207–223. https://doi.org/10.1016/j.epsl.2017.07.015

Lindström, S., van de Schootbrugge, B., Hansen, K. H., Pedersen, G. K., Alsen, P., Thibault, N., Dybkjær, K., Bjerrum, C. J., & Nielsen, L. H. (2017). A new correlation of Triassic–Jurassic boundary successions in NW Europe, Nevada and Peru, and the Central Atlantic Magmatic Province: A time-line for the end-Triassic mass extinction. *Palaeogeography Palaeoclimatology Palaeoecology*, *478*, 80–102. https://doi.org/10.1016/j.palaeo.2016.12.025

Liu, S., Yang, Y., Deng, B., Zhong, Y., Wen, L., Sun, W., Li, Z., Jansa, L., Li, J., Song, J., Zhang, X., & Peng, H. (2021). Tectonic evolution of the Sichuan Basin, Southwest China. *Earth-Science Reviews*, *213*, 103470. https://doi.org/10.1016/j.earscirev.2020.103470

Liu, Z., Li, L., & Wang, Y. (2015). Late Triassic spore-pollen assemblage from Xuanhan of Sichuan, China. *Acta Micropalaeontologica Sinica*, *32*(1), 43–62. https://doi.org/10.16087/j.cnki.1000-0674.20150407.006

Lu, N. (2019). *Changes in sedimentary environment and terrestrial paleoecology across the Triassic-Jurassic transition in eastern Sichuan Basin*, Doctoral thesis, University of Science and Technology of China.

Lu, N., Li, Y., Wang, Y., Xu, Y., & Zhou, N. (2021). Fossil dipterid fern *Thaumatopteris* in China: New insights of systematics, diversity and tempospatial distribution patterns. *Historical Biology*, *33*(10), 2316–2329. https://doi.org/10.1080/08912963.2020.1791106

Lu, N., Wang, Y., Popa, M. E., Xie, X., Li, L., Xi, S., et al. (2019). Sedimentological and paleoecological aspects of the Norian–Rhaetian transition (late Triassic) in the Xuanhan area of the Sichuan Basin, Southwest China. *Palaeoworld*, *28*(3), 334–345. https://doi.org/10.1016/j.palwor.2019.04.006

Lu, N., Xie, X., Wang, Y., & Li, L. (2015). The analysis of sedimentary environmental evolution of the T3x/T2l boundary transition in Qilixia of Xuanhan, Sichuan. *Acta Sedimentologica Sinica*, *33*(6), 1149–1158.

Lucas, S. G., & Tanner, L. H. (2015). End-Triassic nonmarine biotic events. *Journal of Palaeogeography*, *4*(4), 331–348. https://doi.org/10.1016/j.jop.2015.08.010

Lucas, S. G., & Tanner, L. H. (2018). The missing mass extinction at the Triassic-Jurassic boundary. In H. T. Lawrence (Ed.), *The Late Triassic World* (pp. 721–785). Springer.

Mander, L., Kürschner, W. M., & McElwain, J. C. (2013). Palynostratigraphy and vegetation history of the Triassic–Jurassic transition in East Greenland. *Journal of the Geological Society*, *170*(1), 37–46. https://doi.org/10.1144/jgs2012-018

Marzoli, A., Bertrand, H., Knight, K. B., Cirilli, S., Buratti, N., Vérati, C., Nomade, S., Renne, P. R., Youbi, N., Martini, R., Allenbach, K., Neuwerth, R., Rapaille, C., Zaninetti, L., & Bellieni, G. (2004). Synchrony of the Central Atlantic magmatic province and the Triassic-Jurassic boundary climatic and biotic crisis. *Geology*, *32*(11), 973. https://doi.org/10.1130/g20652.1

McElwain, J. C., Beerling, D. J., & Woodward, F. I. (1999). Fossil plants and global warming at the Triassic-Jurassic boundary. *Science*, *285*(5432), 1386–1390. https://doi.org/10.1126/science.285.5432.1386

McElwain, J. C., Popa, M. E., Hesselbo, S. P., Haworth, M., & Surlyk, F. (2007). Macroecological responses of terrestrial vegetation to climatic and atmospheric change across the Triassic/Jurassic boundary in East Greenland. *Paleobiology*, *33*(4), 547–573. https://doi.org/10.1666/06026.1

McElwain, J. C., & Punyasena, S. W. (2007). Mass extinction events and the plant fossil record. *Trends in Ecology & Evolution*, *22*(10), 548–557. https://doi.org/10.1016/j.tree.2007.09.003

Metcalfe, I. (2011). Tectonic framework and Phanerozoic evolution of Sundaland. *Gondwana Research*, *19*(1), 3–21. https://doi.org/10.1016/j.gr.2010.02.016

Michalík, J., Lintnerová, O., Gaździcki, A., & Soták, J. (2007). Record of environmental changes in the Triassic–Jurassic boundary interval in the Zliechov Basin, Western Carpathians. *Palaeogeography, Palaeoclimatology, Palaeoecology*, *244*(1), 71–88. https://doi.org/10.1016/j.palaeo.2006.06.024

Olsen, P. E., Kent, D. V., Sues, H. D., Koeberl, C., Huber, H., Montanari, A., Rainforth, E. C., Fowell, S. J., Szajna, M. J., & Hartline, B. W. (2002). Ascent of dinosaurs linked to an iridium anomaly at the Triassic-Jurassic boundary. *Science*, *296*(5571), 1305–1307. https://doi.org/10.1126/science.1065522

Parrish, J. T., & Peterson, F. (1988). Wind directions predicted from global circulation models and wind directions determined from eolian sandstones of the western United States-a comparison. *Sedimentary Geology*, *56*(1–4), 261–282.

Percival, L. M. E., Ruhl, M., Hesselbo, S. P., Jenkyns, H. C., Mather, T. A., & Whiteside, J. H. (2017). Mercury evidence for pulsed volcanism during the end-Triassic mass extinction. *Proceedings of the National Academy of Sciences*, *114*(30), 7929–7934. https://doi.org/10.1073/pnas.1705378114

Philippe, M., Jiang, H. E., Kim, K., Oh, C., Gromyko, D., Harland, M., Paik, I. S., & Thévenard, F. (2009). Structure and diversity of the Mesozoic wood genus Xenoxylon in Far East Asia: Implications for terrestrial palaeoclimates. *Lethaia*, *42*(4), 393–406. https://doi.org/10.1111/j.1502-3931.2009.00160.x

Philippe, M., & Thévenard, F. (1996). Repartition and palaeoecology of the Mesozoic wood genus Xenoxylon: Palaeoclimatological implications for the Jurassic of Western Europe. *Review of Palaeobotany and Palynology*, *91*(1–4), 353–370. https://doi.org/10.1016/0034-6667(95)00067-4

Pole, M., Wang, Y., Dong, C., Xie, X., Tian, N., Li, L., Zhou, N., Lu, N., Xie, A., & Zhang, X. (2018). Fires and storms—A Triassic–Jurassic transition section in the Sichuan Basin, China. *Palaeobiodiversity and Palaeoenvironments*, *98*(1), 29–47. https://doi.org/10.1007/s12549-017-0315-y

Raup, D. M., & Sepkoski, J. J. (1982). Mass extinctions in the marine fossil record. *Science*, *215*(4539), 1501–1503. https://doi.org/10.1126/science.215.4539.1501

Ruhl, M., Bonis, N. R., Reichart, G.-J., Damsté, J. S. S., & Kürschner, W. M. (2011). Atmospheric carbon injection linked to end-triassic mass extinction. *Science*, *333*(6041), 430–434. https://doi.org/10.1126/science.1204255

Ruhl, M., Hesselbo, S. P., Al-Suwaidi, A., Jenkyns, H. C., Damborenea, S. E., Manceñido, M. O., Storm, M., Mather, T. A., & Riccardi, A. C. (2020). On the onset of Central Atlantic Magmatic Province (CAMP) volcanism and environmental and carbon-cycle change at the Triassic–Jurassic transition (Neuquén Basin, Argentina). *Earth-Science Reviews*, *208*, 103229. https://doi.org/10.1016/j.earscirev.2020.103229

Schoepfer, S. D., Shen, J., Sano, H., & Algeo, T. J. (2022). Onset of environmental disturbances in the Panthalassic Ocean over one million years prior to the Triassic-Jurassic boundary mass extinction. *Earth-Science Reviews*, *224*, 103870.

Sepkoski, J. J. (1981). A factor analytic description of the phanerozoic marine fossil record. *Paleobiology*, *7*(1), 36–53.

Shen, J., Yin, R., Zhang, S., Algeo, T. J., Bottjer, D. J., Yu, J., Xu, G., Penman, D., Wang, Y., Li, L., Shi, X., Planavsky, N. J., Feng, Q., & Xie, S. (2022). Intensified continental chemical weathering and carbon-cycle perturbations linked to volcanism during the Triassic–Jurassic transition. *Nature Communications*, *13*, 299. https://doi.org/10.1038/s41467-022-27965-x

Song, Y., Algeo, T. J., Wu, W., Luo, G., Li, L., Wang, Y., & Xie, S. (2020). Distribution of pyrolytic PAHs across the Triassic-Jurassic boundary in the Sichuan Basin, southwestern China: Evidence of wildfire outside the Central Atlantic Magmatic Province. *Earth-Science Reviews*, *201*, 102970. https://doi.org/10.1016/j.earscirev.2019.102970

Stanley, G. D., Jr., Shepherd, H. M. E., & Robinson, A. J. (2018). Paleoecological response of corals to the end-Triassic mass extinction: An integrational analysis. *Journal of Earth Science*, *29*(4), 879–885. https://doi.org/10.1007/s12583-018-0793-5

Steinthorsdottir, M., Woodward, F. I., Surlyk, F., & McElwain, J. C. (2012). Deep-time evidence of a link between elevated CO_2 concentrations and perturbations in the hydrological cycle via drop in plant transpiration. *Geology*, *40*(9), 815–818. https://doi.org/10.1130/g33334.1

Sun, G., Meng, F., Qian, L., & Ouyang, S. (1995). Triassic floras. In X. Li (Ed.), *Fossil floras of China through the geological ages* (pp. 305–342). Guangdong Science and Technology Press.

Tian, N., Wang, Y., Philippe, M., Li, L., Xie, X., & Jiang, Z. (2016). New record of fossil wood *Xenoxylon* from the late Triassic in the Sichuan Basin, southern China and its paleoclimatic implications. *Palaeogeography, Palaeoclimatology, Palaeoecology*, *464*, 65–75. https://doi.org/10.1016/j.palaeo.2016.02.006

Tomašových, A., & Siblík, M. (2007). Evaluating compositional turnover of brachiopod communities during the end-Triassic mass extinction (northern calcareous Alps): Removal of dominant groups, recovery and community reassembly. *Palaeogeography, Palaeoclimatology, Palaeoecology*, *244*(1), 170–200. https://doi.org/10.1016/j.palaeo.2006.06.028

Van de Schootbrugge, B., Quan, T. M., Lindström, S., Püttmann, W., Heunisch, C., Pross, J., et al. (2009). Floral changes across the Triassic/Jurassic boundary linked to flood basalt volcanism. *Nature Geoscience*, *2*(8), 589–594. https://doi.org/10.1038/ngeo577

Wang, C., Zheng, R., Li, S., Li, S., Li, G., et al. (2017). Stratigraphic subdivision and correlation of the upper Triassic Xujiahe formation, eastern Sichuan Basin: A case study of the Woxinshuang area. *Journal of Stratigraphy*, *41*(1), 94–102.

Wang, J. (1990). Anxian Tectonic Movement. *Oil & Gas Geology*, *11*(3), 223–234.

Wang, J. (2003). Recognition on the main episode of Indo-China movement in the Longmen Moutains. *Acta Geologica Sichuan*, *23*(2), 65–69.

Wang, Y., Fu, B., Xie, X., Huang, Q., Li, K., Li, G., et al. (2010). *The terrestrial Triassic and Jurassic Systems in the Sichuan Basin, China*. University of Sicence and Technology of China Press.

Wang, Y., Li, L. Q., Guignard, G., Dilcher, D. L., Xie, X., Tian, N., et al. (2015). Fertile structures with in situ spores of a dipterid fern from the Triassic in southern China. *Journal of Plant Research*, *128*(3), 445–457. https://doi.org/10.1007/s10265-015-0708-9

Whiteside, J. H., Olsen, P. E., Eglinton, T., Brookfield, M. E., & Sambrotto, R. N. (2010). Compound-specific carbon isotopes from Earth's largest flood basalt eruptions directly linked to the end-Triassic mass extinction. *Proceedings of the National Academy of Sciences of the United States of America*, *107*(15), 6721–6725. https://doi.org/10.1073/pnas.1001706107

Williford, K. H., Foriel, J., Ward, P. D., & Steig, E. J. (2009). Major perturbation in sulfur cycling at the Triassic-Jurassic boundary. *Geology*, *37*(9), 835–838. https://doi.org/10.1130/g30054a.1

Wotzlaw, J. F., Guex, J., Bartolini, A., Gallet, Y., Krystyn, L., McRoberts, C. A., Taylor, D., Schoene, B., & Schaltegger, U. (2014). Towards accurate numerical calibration of the late Triassic: High-precision U-Pb geochronology constraints on the duration of the Rhaetian. *Geology*, *42*(7), 571–574. https://doi.org/10.1130/g35612.1

Wu, S. (1983). On the late Triassic and early-middle Jurassic floras and their distributions in China. In *Palaeobiogeographic provinces of China*, ed. E.C.o.F.T.o.P.B. Series (pp. 121–130). Beijing: Science Press.

Wu, S. (1999). Upper Triassic plants from Sichuan. *Bulletin of Nanjing Institute of Geology and Palaeontology, Academia Sinica*, *14*, 1–69.

Xu, Y., Popa, M. E., Zhang, T., Lu, N., Zeng, J., Zhang, X., Li, L., & Wang, Y. (2021). Re-appraisal of *Anthrophyopsis* (Gymnospermae): New material from China and global fossil records. *Review of Palaeobotany and Palynology*, *292*, 104475. https://doi.org/10.1016/j.revpalbo.2021.104475

Yager, J. A., West, A. J., Thibodeau, A. M., Corsetti, F. A., Rigo, M., Berelson, W. M., Bottjer, D. J., Greene, S. E., Ibarra, Y., Jadoul, F., Ritterbush, K. A., Rollins, N., Rosas, S., Di Stefano, P., Sulca, D., Todaro, S., Wynn, P., Zimmermann, L., & Bergquist, B. A. (2021). Mercury contents and isotope ratios from diverse depositional environments across the Triassic–Jurassic boundary: Towards a more robust mercury proxy for large igneous province magmatism. *Earth-Science Reviews*, *223*, 103775. https://doi.org/10.1016/j.earscirev.2021.103775

Ye, M., Liu, X., Huang, G., Chen, L., Peng, S., et al. (1986). *Late Triassic and early-middle Jurassic fossil plants from northeastern Sichuan*. Anhui Science and Technology Publishing House.

Zhong, D. (1998). *Paleotethysides of the western Guizhou-Sichuan region*. Science Press.

Zhu, M., Chen, H., Zhou, J., & Yang, S. (2017). Provenance change from the middle to late Triassic of the southwestern Sichuan basin, Southwest China: Constraints from the sedimentary record and its tectonic significance. *Tectonophysics*, *700-701*, 92–107. https://doi.org/10.1016/j.tecto.2017.02.006

Zhou, N., Xu, Y., Li, L., Lu, N., An, P., Popa, M. E., Kürschner, W. M., Zhang, X., & Wang, Y. (2021). Pattern of vegetation turnover during the end-Triassic mass extinction: Trends of fern communities from South China with global context. *Global and Planetary Change*, *205*, 103585. https://doi.org/10.1016/j.gloplacha.2021.103585

SUPPORTING INFORMATION

Additional supporting information can be found online in the Supporting Information section at the end of this article.

How to cite this article: Lu, N., Wang, Y., Xu, Y., Li, L., Xie, X., Popa, M. E., Chen, H., Ruhl, M., & Kürschner, W. M. (2023). Oscillations of a fluvial-lacustrine system and its ecological response prior to the end-Triassic: Evidence from the eastern Tethys region. *Geological Journal*, *58*(3), 1239–1255. https://doi.org/10.1002/gj.4658